IET Generation, Transmission & Distribution

Research Article

IET Journals
The Institution of Engineering and Technology

Hierarchical predictive control scheme for distributed energy storage integrated with residential demand and photovoltaic generation

ISSN 1751-8687
Received on 24th September 2014
Revised on 20th May 2015
Accepted on 16th July 2015
doi: 10.1049/iet-gtd.2014.0908
www.ietdl.org

Ioannis Lampropoulos ✉, *Panagiotis Garoufalis**, *Paul P.J. van den Bosch*, *Wil L. Kling*

Electrical Engineering, Eindhoven University of Technology, Den Dolech 2, 5612 AZ, Eindhoven, The Netherlands
**Present address: Aristotle University of Thessaloniki, 54124 Thessaloniki, Greece*
✉ *E-mail: i.lampropoulos@tue.nl*

Abstract: A hierarchical control scheme is defined for the energy management of a battery energy storage system which is integrated in a low-voltage distribution grid with residential customers and photovoltaic installations. The scope is the economic optimisation of the integrated system by employing predictive control techniques. The approach is based on hierarchical decomposition of the optimisation problem in the time domain by composing a three-level scheduling and control scheme, that is, *day-ahead*, *intra-hour*, and *real-time*, where the initial and final states of each sub-problem are chosen as coordination parameters. The *day-ahead* and the *intra-hour* problems address the interactions with electricity markets during the scheduling phase. The *real-time* algorithm is able to adapt the operation of the battery system according to updated information about market conditions, residential demand, and local generation, and subject to the network capacity and other technical constraints. The simulation scenarios address the interactions with the day-ahead auction and the imbalance settlement system in the Netherlands.

1 Introduction

Energy storage technologies provide feasible options for the integration of renewable energy sources (RES) and the efficient delivery of electrical power. The main drivers for the development of energy storage solutions are market opportunities through energy arbitrage, ancillary services provision, efficiency improvements of generation, transmission and distribution assets, and complementary applications [1]. In [2], the optimal energy storage control problem has been addressed from the perspective of the utility operator, with the objective of minimising costs which are modelled as a function of the grid load. Though, a single functionality or application of energy storage is unlikely to provide economic justification [1], and with the advent of electricity markets, the research focus has been shifted from the central role of the utility operator towards developing storage control strategies and applications for the provision of multiple services across different actors and markets. Emphasis is given on both the active and reactive power management to support trading functions and the provision of ancillary services, including the provision of reserves for imbalance adjustments caused by RES [3], and the compensation of power quality disturbances [4].

On the subject of energy management of grid-connected storage integrated with distributed generation, recent studies have been focused on hierarchical approaches and have emphasised on the necessity of predictive optimisation during the scheduling phase to reach the objective of optimal management in real conditions [5, 6]. Riffonneau *et al.* [6] have highlighted the importance of responsive optimisation close to real-time by adjusting the predictive strategy at each unpredicted disturbance according to actual measurements. Yuan *et al.* [7] have addressed the economic optimisation of energy storage, in combination with large-scale wind energy, and have proposed a stochastic programming method to deal with the forecast error in order to minimise imbalance penalties. Wang *et al.* [8] have proposed a hierarchical two-level storage control algorithm, which is decomposed into a feedforward optimisation-based global tier and a feedback control-based local tier, with the objective of cost minimisation of a residential user under a dynamic pricing scheme. Comparably, in this contribution, a three-level control scheme is proposed. The upper control levels address the forecast-based scheduling of a battery energy storage system (BESS), whereas the lower level addresses the dynamically adaptive operation of the BESS. The objective is the economic optimisation of a district BESS, which is integrated in a low-voltage (LV) grid, to address the provision of multiple services and with explicit focus on two developed markets in the Netherlands. The approach is based on hierarchical time decomposition of the optimisation problem by composing a three-level control scheme. The upper control level addresses the application of energy arbitrage within the setting of the Dutch day-ahead auction, whereas the intermediate and lower control levels address the passive contribution in the Dutch imbalance settlement system. The scheduling strategies for both the upper and intermediate control levels have been studied in stand-alone modes [9, 10]. The novelty is the integration of those two strategies into a hierarchical three-level control scheme, where the upper control levels are complemented by a lower controller which optimises the BESS operation close to real-time according to measured quantities and updated predictions and information, and subject to the network capacity and other technical constraints. The optimisation sub-problems are solved by utilising an internal model of the BESS to schedule the future response of the charging and discharging processes over a prediction horizon, where the initial and final states of each sub-problem are chosen as coordination parameters to account for commitments that are made earlier in time. A model-based approach, involving a prediction horizon, for the real-time management of an integrated system with photovoltaic (PV) generation and energy storage has been proposed in [3], with the objective to minimise economic penalties in the Spanish imbalance settlement system. However, in [3], the authors neglect the impact of the storage system efficiency on the economic performance, whereas the *a priori* energy commitment is assumed to become available via an upper energy management level. In this work, the lower control level is complemented by two upper control levels which address the interactions with electricity markets during the scheduling phase. The main

contributions are in the problem formulation of the hierarchical control scheme, and in an ex-post evaluation of the potential revenues from the specified applications, based on historical market data, and including a sensitivity analysis about the effect of the storage system efficiency. Even though the problem has been specified for the Dutch electricity markets, the general principles that guide the proposed strategies are applicable to a wide range of services provided by energy storage technologies in combination with RES.

The paper is organised as follows. In Section 1, the scope of research is outlined. The case study is presented in Section 2. In Section 3, the methodology is elucidated, and the optimisation problem is mathematically formulated. The revenue analysis follows in Section 4, and the paper ends with conclusions and recommendations.

2 Case study

The case study is about a lithium-ion BESS integrated in a typical LV distribution system with residential customers and PV installations in the Netherlands [11], whereas the battery installation consists of a separate container which is located in a public space. A schematic of the case study is depicted in Fig. 1, whereas the main specifications are listed in Table 1. The underlying business model defines an aggregator company as a service provider who is representing to the electricity markets all the connected entities to the LV bus, that is, the residential customers and the PV installations which are regarded as non-controllable resources, and the BESS which is the only controllable resource. In Fig. 1, four network points (a)–(d) are defined, and power measuring devices are installed at points (a) and (b). In this arrangement, it is possible to determine all relevant power flows in the investigated network. The active power at point (c) and at time t can be calculated, while neglecting network losses, by using

$$P_c(t) = P_a(t) - P_b(t) \tag{1}$$

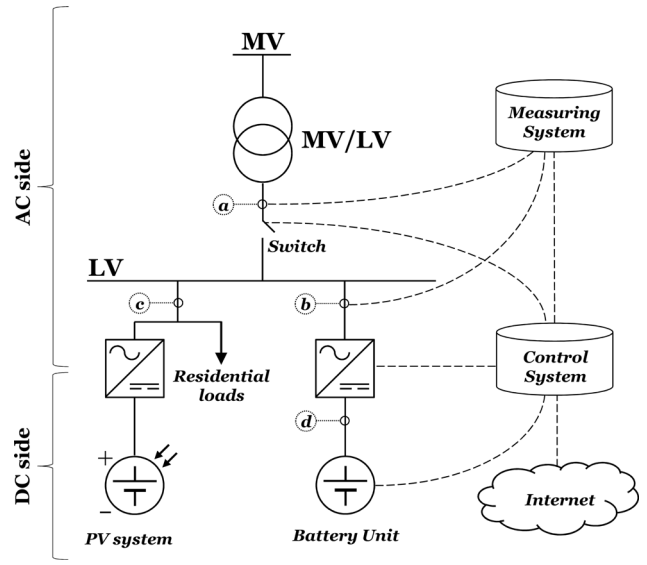

Fig. 1 *Schematic of the case study, illustrating the system setup and the control architecture. The solid black lines depict the physical power network, whereas the dashed lines represent the communication network. Due to bidirectional power flows, by convention it is assumed that power values are positive for the power flows from the MV/LV transformer to the BESS and the residential loads*

Table 1 Case study specifications [11, 12]

Main characteristics	Symbol	Value	Unit
LV distribution system			
Transformer capacity	$\|S_{a,\max}\|$	400	kVA
Maximum net power at point (c)[a]	$P_{c,\max}$	385	kW
Minimum net power at point (c)[a]	$P_{c,\min}$	−50	kW
Number of residencies	—	240	—
Installed PV capacity	—	186	kW_p
Battery energy storage system			
Nominal capacity	E_{nom}	230	kWh
Nominal discharge power	$P_{d,\min}$	−400	kW
Nominal charge power	$P_{d,\max}$	100	kW
Minimum SoE	$\text{SoE}_{\min}$	0.2	—
Maximum SoE	$\text{SoE}_{\max}$	0.9	—

[a]Measured at the end of December 2012.

Under the assumption that the reactive power through the transformer is zero, the capacity constraint related to the installed transformer can be written as follows

$$-400\,\text{kW} - P_c(t) \le P_b(t) \le 400\,\text{kW} - P_c(t) \tag{2}$$

The power conversion system, depicted between points (b) and (d) in Fig. 1, consists of four separate inverter units, each connected to one of the four parallel battery strings, whereas each string is comprised of 29 lithium-ion battery modules in series [12]. An approach to consider the power losses during charging or discharging cycles is by incorporating an estimation of the storage system efficiency

$$P_b(t) = \frac{1}{\eta_{\text{ch}}} \cdot P_{d,\text{ch}}(t) + \eta_{\text{dis}} \cdot P_{d,\text{dis}}(t) \tag{3}$$

where $P_{d,\text{ch}}$, η_{ch}, $P_{d,\text{dis}}$, η_{dis} are the power rates and the efficiency factors during the charging and discharging modes.

3 Optimisation problem formulation

The scope is the economic optimisation of the integrated battery system, that is, the maximisation of profits or minimisation of costs, within the context of certain applications which refer to two developed electricity markets in the Netherlands. The logic is to control the active power at point (b), while accounting for any power deviations at point (c), to shape the exchanging power with the medium-voltage (MV) distribution system at point (a), as depicted in Fig. 1. The realised power transfer with the MV distribution system is subject to contractual trade agreements that occur prior to real-time operations. The approach is through hierarchical decomposition of the optimisation problem in the time domain by composing a three-level control scheme, that is, *day-ahead*, *intra-hour*, and *real-time*.

The hierarchical approach is guided by the nature of the specified problem and the requirements imposed by the design of the considered markets, for example, timescales, timing of procedures, and other associated constraints. The gate closure of the Amsterdam Power Exchange (APX) day-ahead market occurs at noon on the day-ahead, that is, 12 h prior to operations [13], whereas the contribution in system balancing takes place in real-time. Finally, the imbalance and financial settlements occur *a posteriori*, that is, after the operational day. Since the optimisation algorithms utilise as inputs forecasts of market developments, energy generation and demand, solving both the *day-ahead* and the *intra-hour* optimisation sub-problems at the same point in time would compromise the performance of the latter due to the reliance on forecasts which are performed at least 12 h prior to operations. Therefore, the *day-ahead* and the *intra-hour* sub-problems are solved sequentially, so that the latter can take advantage of more accurate forecasts as those become available closer to real-time. An overview of the hierarchical time sequence of the optimisation processes is illustrated in Fig. 2. The three

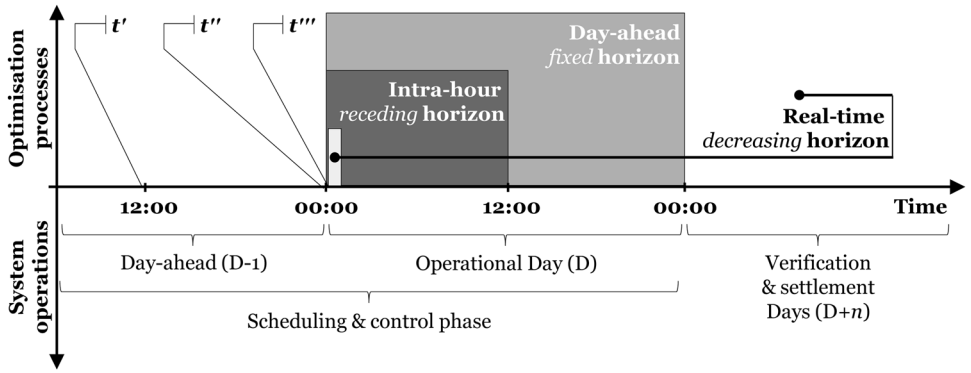

Fig. 2 *Hierarchical time sequence of the optimisation processes for a given day. During the day-ahead, at time instant t′, that is, just before the gate closure time of the day-ahead market at 12:00, the day-ahead optimisation algorithm is executed over a fixed horizon of 24 h (starting at 00:00 of the operational day). At time instant t″, that is, just before the beginning of the operational day, the intra-hour optimisation algorithm is executed for the first time over a receding horizon of 12 h. At time instant t‴, that is, at the first sample time control period (which is considered to be the first minute) of the operational day, the real-time optimisation algorithm is executed for the first time over a decreasing horizon with a fixed endpoint at the end of the current settlement period of 15 min duration*

optimisation sub-problems are solved over different prediction horizons by utilising an internal model of the BESS. All optimisation problems are solved by employing the *global optimisation toolbox* and the *fmincon* function of Matlab. All simulations were performed on a standard computer (Intel Core 2 Duo processor E8500 at 3.16 GHz and 3.46 GB RAM), and the simulation for the *intra-hour* and *real-time* optimisation problems lasted on average <20 s. Therefore, the calculations can be performed fast enough to be implemented in control procedures with a control step of 1 min as proposed in this study. For the revenue analysis in Section 4, the efficiency factors are considered as constants that vary from 0.5 to 1 on the basis of a sensitivity analysis, whereas for the demonstrative examples in this section the efficiency factors during charging and discharging are set to be $\eta_{\text{ch}} = \eta_{\text{dis}} = 0.8$.

3.1 State-space battery model

The state of energy (SoE) of a battery is typically expressed as the ratio of the energy content stored within the battery and its nominal capacity

$$\text{SoE}(t) = \frac{E(t)}{E_{\text{nom}}} \tag{4}$$

where $E(t)$ denotes the battery energy content at time t, and E_{nom} refers to the battery nominal capacity. Considering the BESS as a single input-single output system, a state-space first-order linear model, in discrete-time domain, can be deduced

$$E(t+1) = E(t) + P_d(t) \cdot \tau \tag{5}$$

$$P_d(t) = P_{d,\text{ch}}(t) + P_{d,\text{dis}}(t) \tag{6}$$

$$P_{d,\text{ch}}(t) \cdot P_{d,\text{dis}}(t) = 0 \tag{7}$$

The non-linear constraint expressed in (7) ensures that the BESS is either in charging or discharging mode. For the charging and discharging power limitations, as well as for the SoE limitations, the nominal permissible values are considered (see Table 1)

$$P_{d,\min} \le P_{d,\text{dis}}(t) \le 0 \tag{8a}$$

$$0 \le P_{d,\text{ch}}(t) \le P_{d,\max} \tag{8b}$$

$$\text{SoE}_{\min} \le \text{SoE}(t+1) \le \text{SoE}_{\max} \tag{9}$$

3.2 Day-ahead optimisation

The objective of the *day-ahead* optimisation is to maximise revenues from energy arbitrage in the APX day-ahead market which is based on a two-sided auction model [13]. Assuming certain predictions of the PV generation, the residential demand, and the market clearing prices, the constrained optimisation problem is formulated as the minimisation of a cost function over a finite horizon of 24 h with discrete steps of $\tau_h = 1$ h. During the *day-ahead* scheduling, the aggregator defines an energy schedule $E_a^{\text{das}}(h) = P_a^{\text{das}}(h) \cdot \tau_h$, $h = 1, \ldots, 24$, which is constructed, according to (1), based on the day-ahead prediction of the net PV generation and residential demand $P_c^{\text{das}}(h)$, and the BESS schedule $P_b^{\text{das}}(h)$. The latter is actually an optimised power schedule of the BESS for the hth hour, $h = 1, \ldots, 24$, as the result of the optimisation problem which can be formulated as

$$\min_{P_d^{\text{das}}(h)} \sum_{h=1}^{24} \Theta(h) \tag{10}$$

$$\Theta(h) = E_a^{\text{das}}(h) \cdot \pi^{\text{prd}}(h) \tag{11}$$

$$E_a^{\text{das}}(h) = P_a^{\text{das}}(h) \cdot \tau_h \tag{12}$$

$$P_a^{\text{das}}(h) = P_b^{\text{das}}(h) + P_c^{\text{das}}(h) \tag{13}$$

$$P_b^{\text{das}}(h) = \frac{1}{\eta_{\text{ch}}} \cdot P_{d,\text{ch}}^{\text{das}}(h) + \eta_{\text{dis}} \cdot P_{d,\text{dis}}^{\text{das}}(h) \tag{14}$$

$$E^{\text{das}}(h+1) = E^{\text{das}}(h) + P_d^{\text{das}}(h) \cdot \tau_h \tag{15}$$

$$\text{SoE}^{\text{das}}(h+1) = \frac{E^{\text{das}}(h+1)}{E_{\text{nom}}} \tag{16}$$

where $\Theta(h)$ represents the hourly costs for purchasing an amount of electrical energy $E_a^{\text{das}}(h)$ (in Wh) at a predicted market price $\pi^{\text{prd}}(h)$ (in €/Wh). The optimisation variable $P_d^{\text{das}}(h) = \left\{P_{d,\text{ch}}^{\text{das}}(h), P_{d,\text{dis}}^{\text{das}}(h)\right\}$ refers to the charging $P_{d,\text{ch}}^{\text{das}}(h)$ and discharging $P_{d,\text{dis}}^{\text{das}}(h)$ set-points of the BESS for $h = 1, \ldots, 24$. Constraints (13) and (14)–(16), are derived from (1) and (3)–(5), respectively. Given that $P_c^{\text{das}}(h)$ is considered as a known (i.e. forecasted) parameter, by substituting (11)–(14) in (10), the optimisation problem can be rewritten as

$$\min_{P_d^{\text{das}}(h)} \sum_{h=1}^{24} \left(\frac{1}{\eta_{\text{ch}}} \cdot P_{d,\text{ch}}^{\text{das}}(h) + \eta_{\text{dis}} \cdot P_{d,\text{dis}}^{\text{das}}(h) \right) \cdot \pi^{\text{prd}}(h) \tag{17}$$

subject to constraints for $h \in [1, 24]$

$$P_d^{\text{das}}(h) = P_{d,\text{ch}}^{\text{das}}(h) + P_{d,\text{dis}}^{\text{das}}(h) \tag{18}$$

$$P_{d,\text{ch}}^{\text{das}}(h) \cdot P_{d,\text{dis}}^{\text{das}}(h) = 0 \tag{19}$$

$$P_{d,\min} \leq P_{d,\text{dis}}^{\text{das}}(h) \leq 0 \tag{20a}$$

$$0 \leq P_{d,\text{ch}}^{\text{das}}(h) \leq P_{d,\max} \tag{20b}$$

$$\text{SoE}_{\min} \leq \text{SoE}^{\text{das}}(h+1) \leq \text{SoE}_{\max} \tag{21}$$

$$-400\,\text{kW} - P_c^{\text{das}}(h) \leq \eta_{\text{dis}} \cdot P_{d,\text{dis}}^{\text{das}}(h) \tag{22a}$$

$$\frac{1}{\eta_{\text{ch}}} \cdot P_{d,\text{ch}}^{\text{das}}(h) \leq 400\,\text{kW} - P_c^{\text{das}}(h) \tag{22b}$$

An example of the *day-ahead* optimisation output is provided in Fig. 3*c*. The input data for this particular optimisation are the APX prices depicted in Fig. 3*b*, and the hourly average net power load profile depicted in Fig. 3*a* which is calculated based on measurement data. The aggregator is considered to be an acknowledged market participant that translates the optimised and forecasted profiles into traded hourly energy instruments, that is, purchase and sell contracts for the day-ahead market. The case is assumed to be small enough not to influence the market clearing prices. This is a valid assumption given that the daily volumes concerning the investigated case study correspond to <0.003% of the daily market volumes. In the case that the submitted day-ahead schedule is cleared at market prices, it is automatically transformed into a day-ahead contract $E_a^{\text{dac}}(h) := E_a^{\text{das}}(h)$, with $E_a^{\text{dac}}(h) = P_a^{\text{dac}}(h) \cdot \tau_h$, which dictates the power transfer with the power system during the actual delivery day.

3.3 Intra-hour optimisation

The short-term operational scheduling can be further detailed through the *intra-hour* optimisation. This intermediate control level addresses the passive contribution within the imbalance settlement system of the Netherlands, that is, a voluntary scheme for participation in system balancing which is attributable to the Dutch system organisation [14]. An acknowledged market participant in wholesale trade in the Netherlands has the possibility to voluntarily assist the transmission system operator (TSO) in correcting system imbalances by utilising non-contracted control energy. The Dutch TSO publishes the bid price ladder balancing table [TenneT web-site (bid price ladder balancing): http://energieinfo.tennet.org/Maintenance/RVVBidPriceLadder.aspx?language=en-US], which shows price information for capacity bids offered for balancing, and the balance delta table [TenneT web-site (system balance information): http://www.tennet.org/english/operational_management/System_data_relating_implementation/system_balance_information/index.aspx], which shows the most recent quantities that were requested for its operations. This combined information can be used by market participants to estimate the imbalance settlement prices. The imbalance settlement in the Netherlands is based on the net volumes of provided control energy per settlement period of 15 min [15]. Therefore, the hourly day-ahead energy contract is transformed to a basis of 15 min, typically by dividing the total hourly figures by four, that is, $E_a^{\text{dac}}(l)$, where l is an index for the settlement periods, with $l = 1, \ldots, 96$. Any energy imbalance must be internally solved by the aggregator before the end of the lth settlement period, or settled with the TSO through the imbalance settlement.

The *intra-hour* optimisation utilises as inputs the most recent forecasts with respect to the net local generation and demand, the balancing state of the overall power system, and the imbalance prices. Considering that more accurate forecasts become available closer to real-time, the output of the *intra-hour* optimisation is a refined schedule for the BESS dispatch with the objective to maximise revenues from passive contribution in the Dutch imbalance settlement system, while taking into account any deviation from the day-ahead contract. However, even forecasts that are generated close to real-time will inevitably involve errors. Therefore, the *intra-hour* scheduling is complemented by the lower level *real-time* controller which utilises updated predictions and measured values to reschedule the BESS dispatch.

The *intra-hour* optimisation is performed just before the beginning of each lth settlement period, and covers a receding horizon of 12 h, that is, 48 settlement periods with a duration τ_s of 15 min. The choice of a receding horizon solution was made to account for events that were not initially predicted by the model, whereas the horizon length of 12 h is prescribed by the day-ahead market procedures [13]. The *day-ahead* optimisation is performed just before the market gate closure (around 12:00), and covers the period from 00:00 to 24:00 of the operational day. Therefore, at

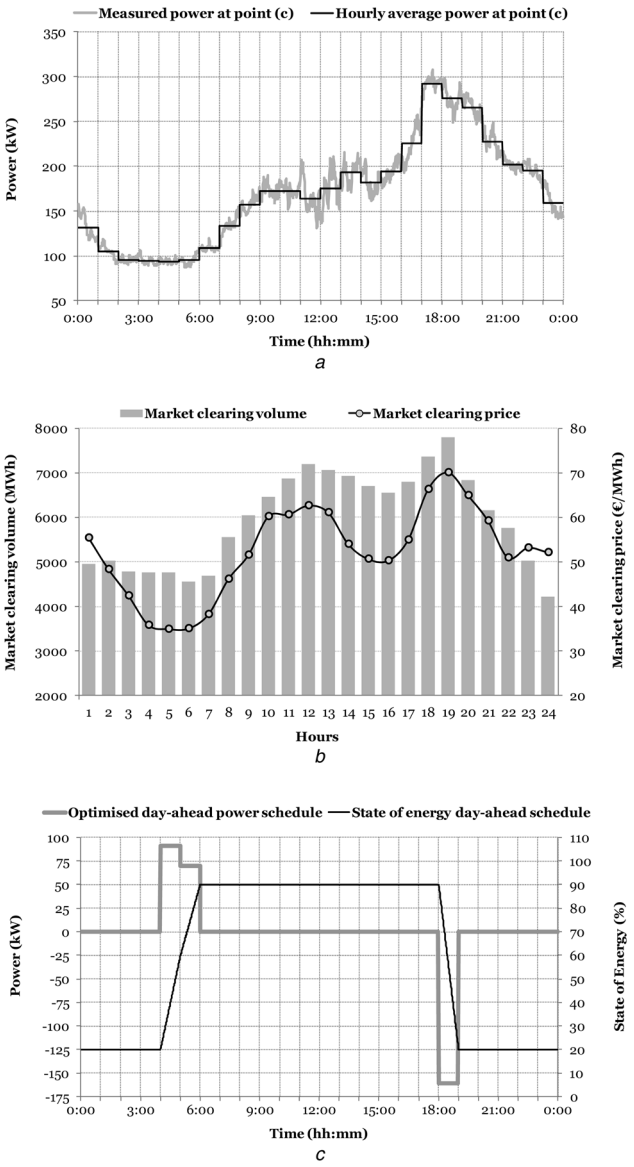

Fig. 3 *Demonstration of the day-ahead optimisation, based on historical data from 1 December 2012*

a Measured and hourly average net power demand and generation of the residential customers and the PV installations

b APX day-ahead market clearing prices and volumes [13]

c Typical output of the *day-ahead* optimisation illustrating the optimised power and SoE schedules of the battery system. The BESS is getting charged until it reaches its maximum allowed SoE, but since it cannot reach the maximum permissible value within 1 hour, due to maximum charging power limitations (≤100 kW), the charging occurs during the 2 hours that correspond to the lowest daily prices, that is, the fifth and sixth hours. Eventually, the battery is getting discharged during the hour that corresponds to the highest daily price, that is, the 19th hour of that day

11:00 of the operational day, the day-ahead contracts are only known for the time period up to 24:00 which implies a maximum horizon of <13 h of known commitments.

Through passive contribution, market participants might try to minimise or maximise their internal energy imbalance during the lth settlement period depending on the system state. The system state $S(l)$ reflects the regulation state of the considered control area during the lth settlement period [15]. Passive contribution can only be identified, and rewarded, for unidirectional dispatch during a settlement period, that is, when $S(l)=1$ (upwards regulation), or $S(l)=-1$ (downwards regulation). On the contrary, passive contribution is not rewarded when the system state is in balance, that is, $S(l)=0$, or when both upwards and downwards regulation is requested during the lth settlement period, that is, $S(l)=2$. Note that market participants face an imbalance price $\pi_{\text{imb}}(l)=\{\pi_{\text{surpl}}(l), \pi_{\text{short}}(l)\}$ which is also dependent on the system state $S(l)$ and the sign of their internal imbalance $\Delta E_a(l)$. The exact price dependencies in the Dutch imbalance settlement can be found in [15]. During the *intra-hour* scheduling, the expected energy imbalance $\Delta E_a^{\text{ihs}}(l)$ for the lth settlement period can be expressed as follows

$$\begin{aligned}\Delta E_a^{\text{ihs}}(l) &= (P_a^{\text{dac}}(l) - P_b^{\text{ihs}}(l) - P_c^{\text{ihs}}(l)) \cdot \tau_{\text{s}} \\ \Leftrightarrow \Delta E_a^{\text{ihs}}(l) &= (-dP_b^{\text{ihs}}(l) - dP_c^{\text{ihs}}(l)) \cdot \tau_{\text{s}}\end{aligned} \tag{23}$$

$$dP_b^{\text{ihs}}(l) = \frac{1}{\eta_{\text{ch}}} \cdot dP_{d,\text{ch}}^{\text{ihs}}(l) + \eta_{\text{dis}} \cdot dP_{d,\text{dis}}^{\text{ihs}}(l) \tag{24}$$

where $P_b^{\text{ihs}}(l) = P_b^{\text{das}}(l) + dP_b^{\text{ihs}}(l)$ is the *intra-hour* optimised power schedule of the BESS, $P_c^{\text{ihs}}(l) = P_c^{\text{das}}(l) + dP_c^{\text{ihs}}(l)$ is the most recent prediction of the net generation and demand at point (c), and $dP_c^{\text{ihs}}(l)$ is the deviation value with respect to the day-ahead schedule. Condition (24) is about the BESS efficiency and is based on (3). Considering the current settlement period $q \in [0, 95]$, the *intra-hour* optimisation objective is the maximisation of a profit function $\Pi(q+m|q)$, $m=1, \ldots, 48$ that represents the expected revenues for the $(q+m)$th settlement periods due to passive contribution

$$\max_{P_d^{\text{ihs}}(q+m|q)} \sum_{m=1}^{48} \Pi(q+m|q) \tag{25}$$

$$\Pi(q+m|q) = \Delta E_a^{\text{ihs}}(q+m|q) \cdot \pi_{\text{imb}}^{\text{prd}}(q+m|q) \tag{26}$$

subject to constraints for $l \in [1, 96]$

$$P_d^{\text{ihs}}(l) = P_{d,\text{ch}}^{\text{ihs}}(l) + P_{d,\text{dis}}^{\text{ihs}}(l) \tag{27}$$

$$P_{d,\text{ch}}^{\text{ihs}}(l) \cdot P_{d,\text{dis}}^{\text{ihs}}(l) = 0 \tag{28}$$

$$P_{d,\,\text{min}} \le P_{d,\text{dis}}^{\text{ihs}}(l) \le 0 \tag{29a}$$

$$0 \le P_{d,\text{ch}}^{\text{ihs}}(l) \le P_{d,\,\text{max}} \tag{29b}$$

$$\text{SoE}_{\text{min}} \le \text{SoE}^{\text{ihs}}(l+1) \le \text{SoE}_{\text{max}} \tag{30}$$

$$-400\,\text{kW} - P_c^{\text{ihs}}(l) \le \eta_{\text{dis}} \cdot P_{d,\text{dis}}^{\text{ihs}}(l) \tag{31a}$$

$$\frac{1}{\eta_{\text{ch}}} \cdot P_{d,\text{ch}}^{\text{ihs}}(l) \le 400\,\text{kW} - P_c^{\text{ihs}}(l) \tag{31b}$$

$$\text{SoE}^{\text{ihs}}(l+48) = \text{SoE}_{\text{ref}}^{\text{ihs}}(l+48) \tag{32}$$

where $\pi_{\text{imb}}^{\text{prd}}(q+m|q)$ refers to the predicted imbalance prices (in €/Wh). The power trajectory $P_d^{\text{ihs}}(q+m|q)$ is the input which satisfies the objective function (25) and refers to the DC charging and discharging power set-points. Constraint (32) reflects the fact that during the *intra-hour* optimisation, the SoE at the end of the optimisation horizon should meet a reference value due to other contractual commitments, for example, day-ahead trade. Therefore, two specific cases can be distinguished. The first case is about the stand-alone *intra-hour* optimisation, and the reference value $\text{SoE}_{\text{ref}}^{\text{ihs}}(l+48)$ is set to be constant at 0.55 which represents the mean value within the nominal permissible SoE range (see Table 1). In the second case, the *intra-hour* optimisation is performed hierarchically, that is, after the *day-ahead* optimisation, and the reference states $\text{SoE}_{\text{ref}}^{\text{ihs}}(l)$ are obtained through linear interpolation from the *day-ahead* optimised energy states $\text{SoE}^{\text{das}}(h)$, which are transformed on a 15 min basis through

$$\begin{aligned}\text{SoE}_{\text{ref}}^{\text{ihs}}(l) = \text{SoE}^{\text{das}}(h) \\ + \frac{\text{SoE}^{\text{das}}(h+1) - \text{SoE}^{\text{das}}(h)}{4} \cdot (l - 1 - 4 \cdot (h-1))\end{aligned} \tag{33}$$

where $l \in [4 \cdot (h-1)+1, 4 \cdot h] \subseteq [1, 96]$ for each hour $h=1, \ldots, 24$.

The output of the *intra-hour* optimisation is an adapted schedule for the BESS, which can be further employed in real-time operations. An example of the *hierarchical* optimisation approach is provided in Fig. 4, where historical data from the 1 December 2012 were utilised as optimisation inputs, but with one exception, the predicted system state for the 40th settlement period, that is, from 09:45 to 10:00, was assumed to be $S^{\text{prd}}(40)=2$, whereas according to the TSO historical data [16], during that period only upward regulation was requested, that is, $S(40)=1$. The reason of manipulating that particular optimisation input is meant for evaluating the algorithm response under erroneous predictions, and this becomes clear in the following paragraphs where the real-time operations are discussed. Fig. 4*a* depicts the predicted system states, and the hourly and quarter-hourly average power profiles at network point (c). In Fig. 4*b*, the imbalance prices for shortage and surplus, which are assumed to be forecasted, are depicted. The BESS optimised *intra-hour* schedules are depicted in Fig. 4*c*.

3.4 Real-time operations

The lower level controller is tracking any energy deviations from the day-ahead contract, while taking into account the optimised profiles of the *intra-hour* optimisation. The *real-time* optimisation is performed within each settlement period of the balancing market, and over a decreasing prediction horizon with a fixed endpoint at the end of the settlement period. The sample time interval is set to $\tau=1$ min, and at each time interval the controller receives updated predictions and measured values, and reschedules the charging and discharging processes over the prediction horizon, subject to the expected economic impact and technical constraints. The choice of a decreasing prediction horizon for the *real-time* optimisation is guided by the nature of the specified application, since the imbalance settlement in the Netherlands is performed separately for each settlement period [15]. Therefore, during real-time operations, the aggregator has to comply with the *a priori* defined day-ahead power contract $P_a^{\text{dac}}(l)$ for the lth settlement period, $l=1, \ldots, 96$, whereas any mismatch will be regarded as an energy imbalance $\Delta E_a(l)$

$$\begin{aligned}\Delta E_a(l) &= P_a^{\text{dac}}(l) \cdot \tau_{\text{s}} - \sum_{t=i_l}^{i_{l+1}-1} P_a^{\text{msr}}(t) \cdot \tau \\ &= (P_a^{\text{dac}}(l) - P_a^{\text{msr}}(l)) \cdot \tau_{\text{s}}\end{aligned} \tag{34}$$

where $P_a^{\text{msr}}(t)$ is the measured power at point (a) and at time t, with $t \in [i_l,\ i_{l+1}-1]$ for each $l \in [1, 96]$, whereas $i_l = 15 \cdot (l-1)+1$ corresponds to the first sample time period of the lth settlement period. At current time k any expected energy imbalance by the end of the lth settlement period can be expressed through an

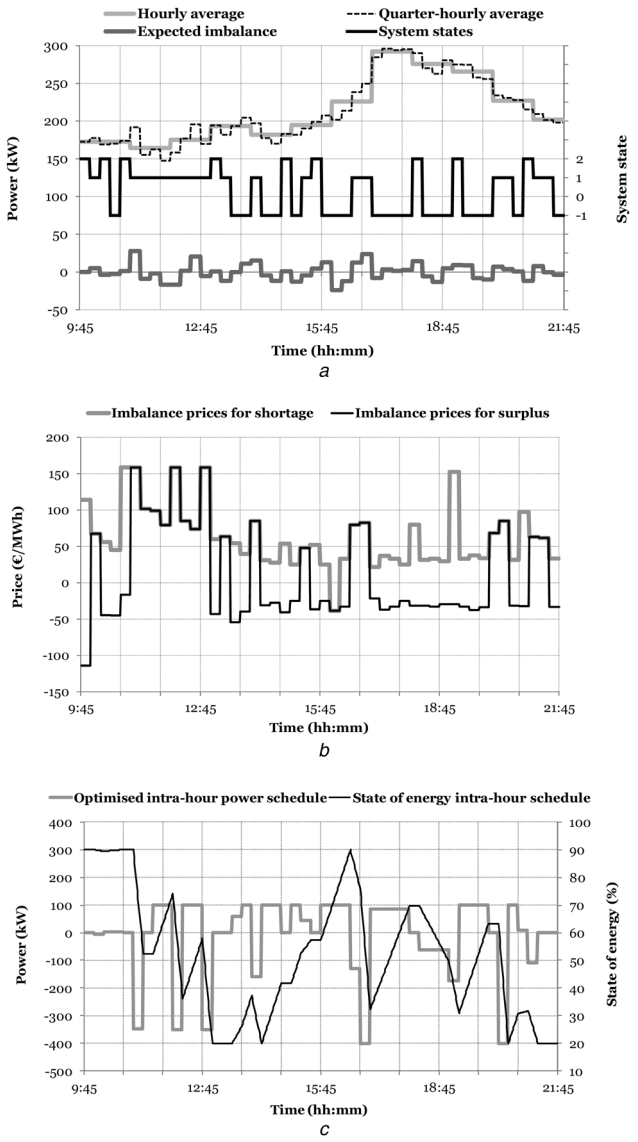

Fig. 4 *Demonstration of the intra-hour optimisation based on data from 1 December 2012*

a Hourly and quarter-hourly average net power profiles for the residential demand and the PV generation, the expected power imbalance, and the predicted system states. These average power profiles have been calculated based on actual field measurements and are utilised as optimisation inputs to resemble the day-ahead schedule $P_c^{\text{das}}(h)$, that is, the hourly average profile, and the intra-hour forecast $P_c^{\text{ihs}}(l)$, that is, the quarter-hourly average profile. After subtraction of the hourly average profile from the quarter-hourly average profile, the resulted power imbalance is assumed to be the expected imbalance $dP_c^{\text{ihs}}(l)$

b Predicted imbalance prices for shortage and surplus of energy

c Optimised *intra-hour* schedules for the BESS. At the end of the prediction horizon, that is, at 21:45, the SoE arrives at the reference value $\text{SoE}_{\text{ref}}^{\text{ihs}}(88) = 0.2$, according to the day-ahead schedule and condition (32)

energy balance equation which is based on (34)

$$\Delta E_a^{\text{rts}}(l|k) = P_a^{\text{dac}}(l)\cdot\tau_{\text{s}} - \sum_{t=15\cdot(l-1)+1}^{k} P_a^{\text{msr}}(t)\cdot\tau - \sum_{i=1}^{15\cdot l-k} P_a^{\text{rts}}(k+i|k)\cdot\tau \tag{35}$$

where the first term in (35) represents the energy volume which has been cleared at the wholesale level for the lth settlement period, the second term represents the accumulated energy content up to current time k (based on actual measurements since the beginning of the lth settlement period, that is, $P_a^{\text{msr}}(t)$ for $t \le k$), and the third term represents the expected accumulated energy from current time k until the end of the lth settlement period. The notation $P_a^{\text{rts}}(k+i|k)$ indicates that the power trajectory depends on the conditions at time k. In real-time, the aggregator coordinates the future response of the BESS by determining a set-point power trajectory that the BESS output should follow from current time k and until the end of the lth settlement period. This set-point power trajectory $P_b^{\text{rts}}(k+i|k)$, for $i = 1, \ldots, 15\cdot l - k$ can be calculated by using (36)

$$\Delta E_a^{\text{rts}}(l|k) = P_a^{\text{dac}}(l)\cdot\tau_{\text{s}} - \sum_{t=15\cdot(l-1)+1}^{k} P_a^{\text{msr}}(t)\cdot\tau - \sum_{i=1}^{15\cdot l-k}\left(P_c^{\text{rts}}(k+i|k) + P_b^{\text{rts}}(k+i|k)\right)\cdot\tau \tag{36}$$

$$P_b^{\text{rts}}(k+i|k) = P_b^{\text{das}}(k+i) + dP_b^{\text{rts}}(k+i|k) \tag{37}$$

$$P_c^{\text{rts}}(k+i|k) = P_c^{\text{das}}(k+i) + dP_c^{\text{rts}}(k+i|k) \tag{38}$$

$$dP_b^{\text{rts}}(k+i|k) = \frac{1}{\eta_{\text{ch}}}\cdot dP_{d,\text{ch}}^{\text{rts}}(k+i|k) + \eta_{\text{dis}}\cdot dP_{d,\text{dis}}^{\text{rts}}(k+i|k) \tag{39}$$

$$P_{d,\text{ch}}^{\text{rts}}(k+i|k) = P_{d,\text{ch}}^{\text{das}}(k+i) + dP_{d,\text{ch}}^{\text{rts}}(k+i|k) \tag{40}$$

$$P_{d,\text{dis}}^{\text{rts}}(k+i|k) = P_{d,\text{dis}}^{\text{das}}(k+i) + dP_{d,\text{dis}}^{\text{rts}}(k+i|k) \tag{41}$$

where $P_b^{\text{rts}}(k+i|k)$ is the *real-time* optimised power trajectory, $P_b^{\text{das}}(k+i)$ reflects the power set-point defined during the *day-ahead* optimisation, that is, $P_b^{\text{das}}(h)$, whereas $dP_b^{\text{rts}}(k+i|k)$ is a power adjustment trajectory for the BESS which is defined in real-time. The real-time schedule $P_c^{\text{rts}}(k+i|k)$ is a power trajectory forecast of the combined residential demand and PV generation over the prediction horizon. The *real-time* optimisation objective is the maximisation of a profit function Λ over a decreasing horizon

$$\max_{dP_d^{\text{rts}}(k+i|k)} \Lambda(k+i|k), \text{ with } i = 1, \ldots, 15\cdot l - k \tag{42}$$

$$\Lambda(k+i|k) = \Delta E_a^{\text{rts}}(l|k)\cdot\pi_{\text{imb}}^{\text{prd}}(l) + \left(\text{SoE}^{\text{rts}}(t = 15\cdot l + 1) - \text{SoE}^{\text{ihs}}(l+1)\right)\cdot E_{\text{nom}}\cdot\pi_{\text{imb}}^{\text{prd}}(l+1) \tag{43}$$

subject to constraints for $t \in [i_l,\ i_{l+1} - 1]$

$$P_d^{\text{rts}}(t) = P_{d,\text{ch}}^{\text{rts}}(t) + P_{d,\text{dis}}^{\text{rts}}(t) \tag{44}$$

$$P_{d,\text{ch}}^{\text{rts}}(t)\cdot P_{d,\text{dis}}^{\text{rts}}(t) = 0 \tag{45}$$

$$P_{d,\min} \le P_{d,\text{dis}}^{\text{rts}}(t) \le 0 \tag{46a}$$

$$0 \le P_{d,\text{ch}}^{\text{rts}}(t) \le P_{d,\max} \tag{46b}$$

$$\text{SoE}_{\min} \le \text{SoE}^{\text{rts}}(t+1) \le \text{SoE}_{\max} \tag{47}$$

$$-400\,\text{kW} - P_c^{\text{rts}}(t) \le \eta_{\text{dis}}\cdot P_{d,\text{dis}}^{\text{rts}}(t) \tag{48a}$$

$$\frac{1}{\eta_{\text{ch}}}\cdot P_{d,\text{ch}}^{\text{rts}}(t) \le 400\,\text{kW} - P_c^{\text{rts}}(t) \tag{48b}$$

where $\pi_{\text{imb}}^{\text{prd}}(l)$ is the predicted imbalance price (in €/Wh) for the lth settlement period, and $dP_d^{\text{rts}}(k+i|k)$ with $i = 1, \ldots, 15\cdot l - k$ is the input trajectory which satisfies the objective function (42) and refers to the DC charging (or discharging) power adjustment trajectory. Constraints (44)–(47) are derived from (6)–(9), respectively, whereas (48) is based on (2). The first term in (43) reflects the expected revenues to be obtained through the imbalance settlement system for the lth settlement period, whereas the second term is meant to penalise any deviation from the expected optimised intra-hour state $\text{SoE}^{\text{ihs}}(l+1)$ at the end of the lth settlement period, that is, the horizon fixed endpoint. For instance, if the predicted state of the $(l+1)$th settlement period indicates a request for upwards regulation, and a positive deviation

of the SoE at the end of the prediction horizon is expected, that is, $(\mathrm{SoE}^{\mathrm{rts}}(15 \cdot l + 1) - \mathrm{SoE}^{\mathrm{ihs}}(l + 1)) > 0$, then this additional amount of energy stored in the BESS is available for discharging purposes, and should be rewarded. On the contrary, if a negative energy deviation is expected, that is, $(\mathrm{SoE}^{\mathrm{rts}}(15 \cdot l + 1) - \mathrm{SoE}^{\mathrm{ihs}}(l + 1)) < 0$, then the imbalance price at the subsequent period should represent an economic penalty. The output of the *real-time* algorithm consists of optimised power set-points and corresponding energy states over the prediction horizon. Note that the optimised value $\mathrm{SoE}^{\mathrm{rts}}(15 \cdot l + 1)$, which results from the last iteration of the *real-time* algorithm within the lth settlement period, is applied as an input to the *intra-hour* optimisation for the subsequent $(l + 1)$th settlement period.

To demonstrate the real-time operation, and the time sequence of actions involved within the proposed hierarchical approach, an illustrative example is given in Fig. 5, whereas the focus is on the 40th settlement period, that is, from 09:45 to 10:00. According to the TSO historical data [16], during that period only upward regulation was requested. However, for this example, it is assumed that the predicted system state $S^{\mathrm{prd}}(l)$ for the lth settlement period, which subsequently influences the imbalance price, involves errors. Thus, it is of interest to observe the capability of the optimisation algorithm to adapt the BESS schedule while updated forecasts become available.

As illustrated in Fig. 5*a*, the first forecast that is utilised as input in the *intra-hour* algorithm, becomes available just before the beginning of the 40th settlement period, indicating that during that period both upward and downward regulation will be requested which subsequently implies financial penalties for any passive contribution. Furthermore, according to (23), another optimisation input is the expected energy imbalance $dP_c^{\mathrm{ihs}}(l)$. For this example, the imbalance values $dP_c^{\mathrm{ihs}}(l)$ were assumed to be equal to the difference between the hourly average and the quarter-hourly average profiles. As can be seen in Fig. 4*a*, from 09:45 to 10:00, the assumed energy imbalance $dP_c^{\mathrm{ihs}}(40)$ is almost negligible, ca. 0.02 kWh. Therefore, given that the predicted system state implies penalties for any internal imbalance, it is a rational decision to maintain the BESS in idle mode. This is illustrated in Figs. 4*c* and 5*b*, where the first step of the *intra-hour* optimisation output is applied at the first minute of the 40th settlement period and commands neither a charging nor a discharging set-point for the BESS. Subsequently, the updated system state forecast becomes available, that is, before 09:46, indicating that the system state for the 40th period will be explicitly for upward regulation, and the output of the *real-time* optimisation defines a discharging set-point at the maximum nominal value, to maximise revenues from passive contribution. The subsequent updated forecast becomes available before 09:50, indicating again that during the 40th period both upward and downward regulation will be requested, thus penalising any imbalance with respect to the day-ahead contract. Therefore, the controller commands the BESS to stop discharging and to start charging at the maximum nominal value, to compensate for the internal imbalance created from 9:46 to 9:50. Finally, before 09:55, the last updated forecast becomes available, indicating that the system state for the 40th period will be explicitly for upward regulation, and the BESS is commanded to get discharged at the maximum nominal value, to maximise revenues from passive contribution. This example illustrates the ability of the lower control level to adapt the output of the BESS when updated forecasts become available close to real-time. This is an essential feature for systems operating within stochastic environments characterised by uncertain conditions.

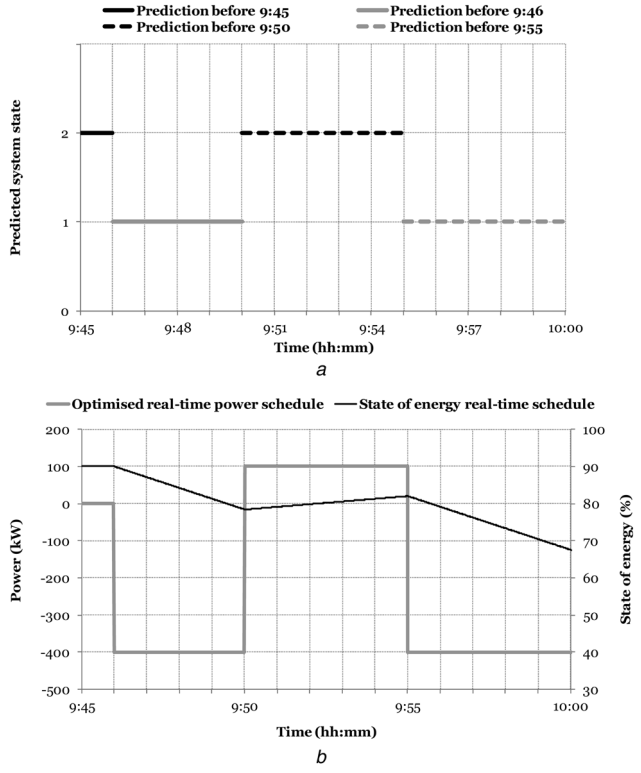

Fig. 5 *Demonstration of the real-time operations, under the hierarchical optimisation approach, based on data from 1 December 2012*

a Predicted system states as those are assumed to become available at subsequent time instants and close to real-time. For this example, it is assumed that from 09:45 to 10:00, the forecasts regarding the predicted system state for the 40th settlement period were updated (changed) four times

b Optimised real-time operation of the BESS in response to updated forecasts regarding the system state

4 Revenue analysis and results

A revenue analysis is performed on the basis of an ex-post evaluation of the specified applications based on historical market data. Therefore, the computed revenues reflect the theoretical maximum that could be achieved for each specified application separately (stand-alone modes) and in combination (hierarchically). For the *day-ahead* optimisation, historical data of the APX day-ahead market, from 2000 to 2012, were utilised [13], whereas for the *intra-hour* optimisation the input consisted of historical data from the Dutch imbalance settlement for the period from 2001 to 2012 [16]. Emphasis is given on the effect of the storage system efficiency, which significantly impacts the overall economic performance due to energy losses during charging and discharging cycles.

4.1 Day-ahead optimisation

The *day-ahead* optimisation results are presented in Fig. 6*a*. Overall, the computed revenues are declining, throughout the years, but this is also the case for the historical price volatility in the APX day-ahead market [9], thus suggesting that market opportunities for energy storage are decreasing with respect to the specified application.

4.2 Intra-hour optimisation

The results of the stand-alone *intra-hour* optimisation are depicted in Fig. 6*b*. The random distribution of maximum annual revenues is governed by the development of system states and imbalance prices throughout the years. The development of the system state and the amplitude of imbalances are driven by a number of factors related to cross-border trade, weather phenomena, and the portfolios of energy service providers, whereas the imbalance price development is also driven by the bid strategies of ancillary services providers. Passive contribution in system balancing can be an additional source of revenues for decentralised market participants, though, the provision of control energy through passive contribution is delivered at the participant's own risk and might jeopardise any contractual payments [10].

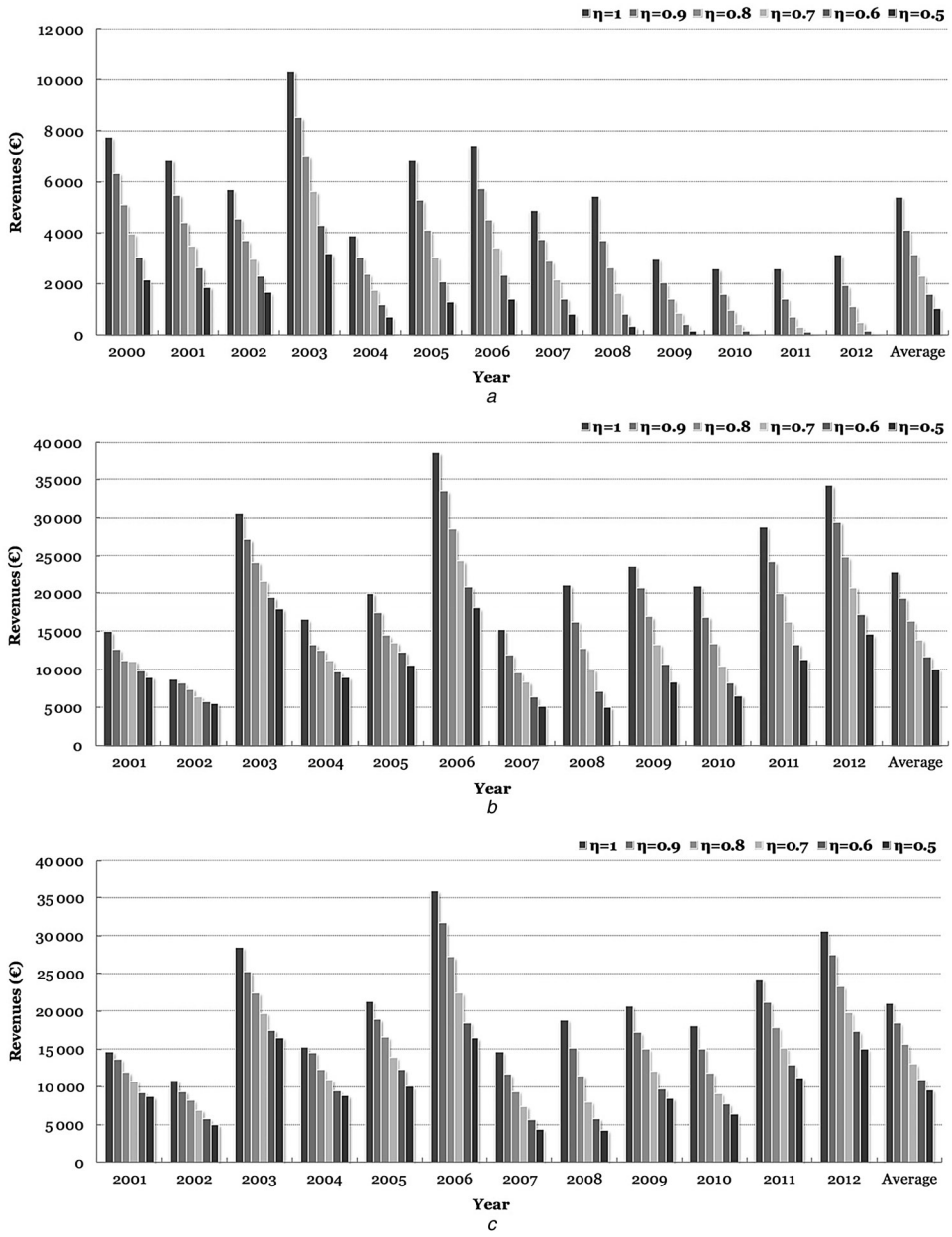

Fig. 6 *Computed maximum annual revenues for varying charging and discharging efficiency factors*

a Exclusive participation in the APX day-ahead market, that is, stand-alone *day-ahead* optimisation

b Exclusive passive contribution in the Dutch imbalance settlement system, that is, stand-alone *intra-hour* optimisation

c Combined energy arbitrage in the day-ahead market and passive contribution in the Dutch imbalance settlement system when part of the capacity has been committed for the day-ahead market, that is, *hierarchical* optimisation approach. Simulation results show that the average computed revenues for the case of the *hierarchical* optimisation approach are slightly less compared with the case of the stand-alone *intra-hour* optimisation, and this is mostly related to the larger price spread observed in the imbalance market, compared with the day-ahead market. However, the risks associated with the imbalance market are higher due to its stochastic nature and the inherent difficulty to accurately predict the imbalance prices and system states *a priori*. Therefore, through the *hierarchical* optimisation approach, the associated risks can be considerably compensated by giving preference to participation in the day-ahead market that is characterised by a diurnal pattern of prices and which makes the forecasting of day-ahead market prices more plausible

4.3 Hierarchical optimisation

In the case of *hierarchical* optimisation, the output of the *day-ahead* optimisation is employed as input in the *intra-hour* optimisation. This results to additional constraints for the *intra-hour* optimisation due to day-ahead commitments. Insight on the hierarchical approach can be given by evaluating the combined computed revenues from both applications. In Fig. 6*c*, the computed maximum annual revenues are depicted for the case of the *hierarchical* optimisation approach, that is, combined revenues from both energy arbitrage in the day-ahead APX market and passive contribution in the Dutch imbalance settlement system.

In Table 2, the percentage drop of average computed revenues for the years from 2001 to 2012 are summarised for the different strategies and for decreasing efficiency factors. On the basis of these figures, it can be concluded that the application of energy arbitrage on the day-ahead market is highly susceptible to the

Table 2 Percentage drop of average computed revenues from 2001 to 2012 for decreasing efficiency factors

Application	η = 0.9, %	η = 0.8, %	η = 0.7, %	η = 0.6, %	η = 0.5, %
Day-ahead energy arbitrage	24.2	42.0	57.5	70.7	81.0
Imbalance settlement Passive contribution	16.9	26.2	40.9	47.2	57.6
Hierarchical optimisation	18.4	29.7	46.6	57.2	65.3

efficiency of the storage system, which indicates the limited business potential of low efficiency storage technologies.

5 Conclusions and future work

A hierarchical control scheme is defined which addresses the economic optimisation of distributed energy storage systems integrated with intermittent generation and residential demand. Even though the case study is just about an integrated system with battery-based energy storage, local PV generation, and residential customers, the proposed method is applicable to different energy storage technologies and intermittent energy sources. The outcome of computer simulations provides an evaluation of the potential revenue that could be achieved with respect to the specified applications, that is, energy arbitrage in the day-ahead market and passive contribution in system balancing (separately and in combination), based on historical market data from the Netherlands, and including a sensitivity analysis about the effect of the storage system efficiency. Simulation results provided a valuable insight about the different utilisation strategies of the distributed energy storage resource. The application of energy arbitrage in the day-ahead market appears to be highly susceptible to the efficiency of the storage system and the daily price development and volatility. On the contrary, contribution to system balancing appears to be a more profitable strategy, which is mainly driven by the larger price spread in the imbalance settlement, and the opportunity for the controller to perform more charging cycles during a day. However, the latter application involves higher risks due to the stochastic nature of the imbalance market and the inherent difficulty to accurately predict the system state *a priori*, whereas contemporary day-ahead markets are characterised by a diurnal pattern of prices, which makes the forecasting of day-ahead market prices more plausible. A hierarchical approach, that is, combined participation in both markets, appeared to be a less effective strategy since the energy commitments that are made day-ahead might restrict the full potential of the storage resource to maximise revenues in real-time markets. These conclusions are made under the assumption of accurate predictions, by utilising historical market data, therefore, the computed revenues reflect the theoretically maximum values. However, in real-life applications, the potential revenues will always be dependent on the accuracy of the forecasting methods. In future work, it is of interest to investigate the impact of forecast errors on the performance of the proposed control scheme within the context of stochastic optimisation. Given the uncertain environment, it is highly relevant to incorporate an assessment with respect to the confidence levels of each predicted quantity and to employ risk-management techniques to define the future control inputs. The focus was on the problem formulation and the evaluation of the specified applications, and not on obtaining the most efficient solution to the problem. In future work, the non-linear constraint expressed in (7) could be converted into an equivalent linear form to guarantee finite convergence to optimality.

For the potential revenue analysis, the efficiency factors were considered as constants, that is, excluding efficiency dependencies and associated energy losses. This design choice was driven by the research objective of computing the theoretical maximum revenues, thus excluding factors that incur additional loss of revenues such as efficiency and battery-lifetime dependencies, as well as forecast errors. However, in practice, there are many parameters that influence the battery performance such as the charging and discharging power rates and temperature. In [17], the authors show that discharging at 2C rate is about 7% less efficient compared with discharging at 1C rate. Therefore, a more accurate representation of the overall power losses is essential with respect to real-life applications since efficiency dependencies may impact significantly the economic performance.

Finally, the outcome of a revenue analysis alone cannot be considered as conclusive about the economic viability of certain energy storage applications. Emphasis was given on evaluating the potential revenues from the specified applications, although, in a real-life market-based environment the optimisation objective shall reflect the maximisation of profit, that is, the excess of revenue over cost. The dependence of lithium-ion battery degradation on demanding conditions related to depth of discharge, power rates, temperature, and so on can be significant, and models have been proposed for predicting the remaining battery capacity [18], and the battery cycle life [19]. With such knowledge, the economic nature of the proposed optimisation approach can be extended to incorporate costs related to battery usage and reduced lifetime.

6 References

1 Cigre Working Group C6.15: 'Electric energy storage systems' (Cigre, 2011)
2 Koutsopoulos, I., Hatzi, V., Tassiulas, L.: 'Optimal energy storage control policies for the smart power grid'. Proc. of IEEE Int. Conf. on Smart Grid Communications, Brussels, 17–20 October 2011
3 Perez, E., Beltran, H., Aparicio, N., *et al.*: 'Predictive power control for PV plants with energy storage', *IEEE Trans. Sustain. Energy*, 2013, **4**, (2), pp. 482–490
4 Wasiak, I., Pawelek, R., Mienski, R.: 'Energy storage application in low-voltage microgrids for energy management and power quality improvement', *IET Gener. Transm. Distrib.*, 2014, **8**, (3), pp. 463–472
5 Nicolai, S., Ritter, S., Beyer, D., *et al.*: 'A hierarchical management approach for electrical energy storages in distribution grids'. Proc. of IEEE Power and Energy Society General Meeting, San Diego, 22–26 July 2012
6 Riffonneau, Y., Bacha, S., Barruel, F., *et al.*: 'Optimal power flow management for grid connected PV systems with batteries', *IEEE Trans. Sustain. Energy*, 2011, **2**, (3), pp. 309–320
7 Yuan, Y., Li, Q., Wang, W.: 'Optimal operation strategy of energy storage unit in wind power integration based on stochastic programming', *IET Renew. Power Gener.*, 2011, **5**, (2), pp. 194–201
8 Wang, Y., Lin, X., Pedram, M.: 'Adaptive control for energy storage systems in households with photovoltaic modules', *IEEE Trans. Smart Grid*, 2014, **5**, (2), pp. 992–1001
9 Lampropoulos, I., Garoufalis, P., van den Bosch, P.P.J., *et al.*: 'Day-ahead economic scheduling of energy storage'. Proc. of Power Systems Computation Conf., Wroclaw, 18–22 August 2014
10 Lampropoulos, I., Garoufalis, P., Kling, W.L.: 'Scheduling of distributed energy storage for passive contribution in the imbalance settlement system of the Netherlands'. Proc. of Int. Conf. on CIGRÉ Innovation for Secure and Efficient Transmission Grids, Brussels, 12–14 March 2014
11 de Groot, R.J.W., van Overbeeke, F., Schouwenaar, A.J.M., *et al.*: 'Smart storage in the Enexis LV distribution grid'. Proc. of Int. Conf. on Electricity Distribution (CIRED), Stockholm, June 2013
12 Saft: 'User's manual Enexis lithium-ion battery system' (Saft Industrial Battery Group, 2011, edn.)
13 'APX Day-Ahead Auction'. Available at http://www.apxgroup.com/trading-clearing/day-ahead-auction, accessed May 2015
14 TenneT: 'Imbalance management TenneT' (TenneT, E-Bridge, GEN Nederland, 2011)
15 TenneT: 'The imbalance pricing system as at 01-01-2001, revised per 26-10-2005' (TenneT, 2010)
16 'TenneT Data export: Balance delta with prices'. Available at http://www.tennet.org/english/operational_management/export_data.aspx, accessed May 2015
17 Shin, D., Kim, Y., Wang, Y., *et al.*: 'Constant-current regulator-based battery-supercapacitor hybrid architecture for high-rate pulsed load applications', *J. Power Sources*, 2012, **205**, pp. 516–524
18 Rong, P., Pedram, M.: 'An analytical model for predicting the remaining battery capacity of lithium-ion batteries', *IEEE Trans. Very Large Scale Integr. (VLSI) Syst.*, 2006, **14**, (5), pp. 441–451
19 Millner, A.: 'Modeling lithium ion battery degradation in electric vehicles'. Proc. Conf. on Innovative Technologies for an Efficient and Reliable Electricity Supply (CITRES), Waltham, 27–29 September 2010